Supplementary Information

Photosensitisation of Inkjet-Printed Graphene with Stable All-Inorganic Perovskite Nanocrystals

Jonathan S. Austin, Nathan D. Cottam, Chengxi Zhang, Feiran Wang, Jonathan H. Gosling, Oliver Nelson-Dummet,[a] Tyler S. S. James, Peter H. Beton, Christopher J. Tuck, Richard Hague, Oleg Makarovsky and Lyudmila Turyanska

SI1. Morphological and optical characterization of perovskite NCs

High resolution transmission electron microscopy (HR TEM) images revealed that the $CsPb(X)_3$ perovskite NCs have hexagonal shape and a diameter of 11 ± 1 nm (analysed by ImageJ: https://imagej.nih.gov/). A representative TEM image and a histogram of the size distribution is shown in the Figure S1. The NCs are stable with respect to optical properties for a period of at least two month (Figure S2). A small (< 10%) decay of PL intensity is recorded.

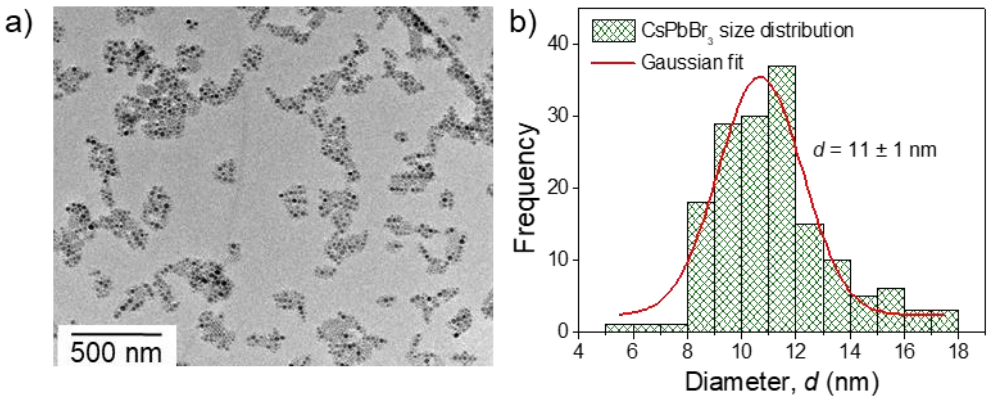

Figure S1 a) A representative TEM image of $CsPbBr_3$ NCs. **b)** Histogram of the size distribution of $CsPbBr_3$ perovskite nanocrystals.

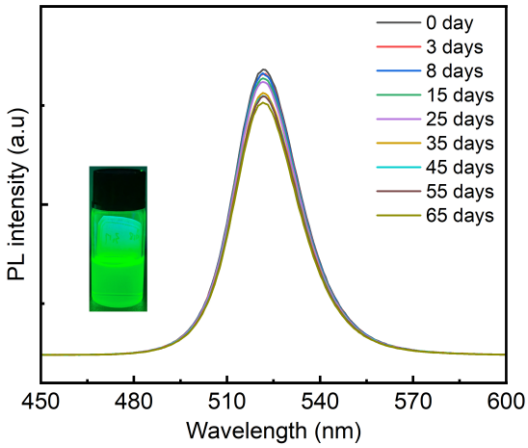

Figure S2 PL spectra of $CsPb(Br)_3$ NCs recorded at different timepoint over a period of two month.

SI2. Photoluminescence (PL) mapping and atomic force microscopy (AFM) of printed perovskite NC films

PL mapping was used to assess the optical properties of $CsPbBr_3$ NC films with 1 and 2 printed layers, and 2 printed layers annealed at 100 °C (Figure S3a). No change in PL properties was observed for the 3 samples (Figure S3b), indicating that the optical properties of the NCs are unchanged after annealing. For a single printed layer, PL mapping revealed a uniform emission with a factor of 2 difference between the maximum and minimum PL intensity coinciding with the edges of individual printed lines (Figure S3c). An increase in uniformity was observed for the film with 2 printed layers (Figure S3d) with no significant change in PL after annealing at 100 °C (Figure S3e). The non-uniformity is well correlated with the printing strategy used [S1].

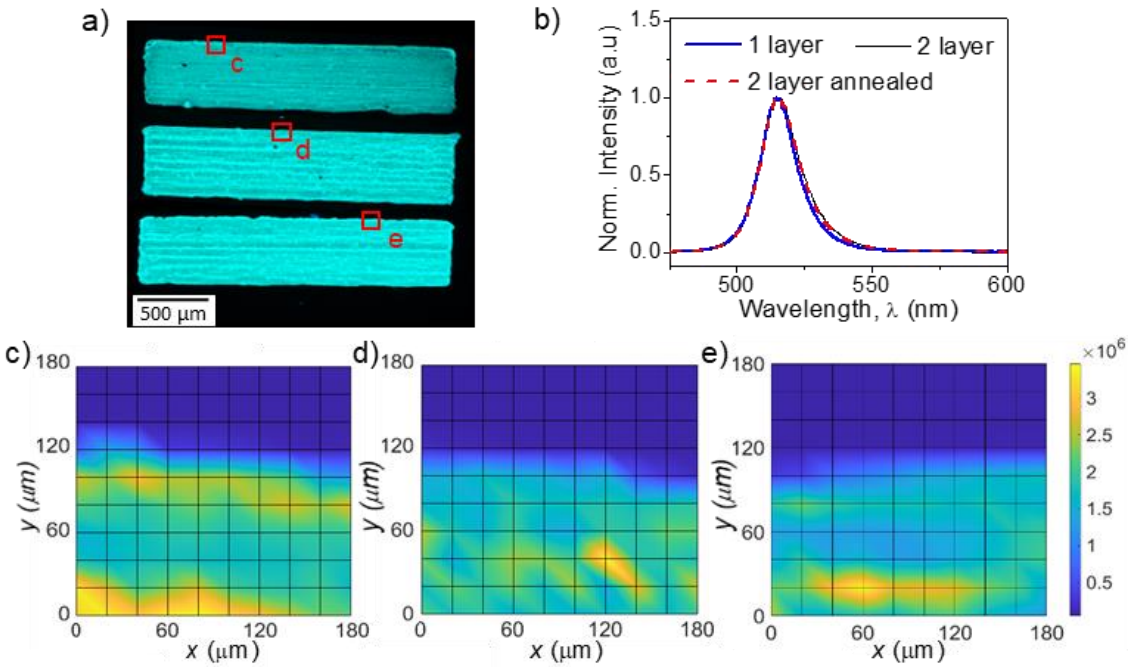

Figure S3 a) Representative optical images of $CsPbBr_3$ NC films under UV illumination (λ_{ex} = 365 nm). The top image shows 1 printed layer, middle image shows 2 printed layers and bottom image shows 2 printed layers annealed at 100 °C for 30 minutes. **b)** Normalised PL spectra from each of the studied $CsPbBr_3$ films shown in a). Map of PL emission for **c)** 1 layer, **d)** 2 layers and **e)** 2 annealed layers of perovskite NCs.

AFM was used to determine the thickness and roughness of printed perovskite NC films. For five printed layers of $CsPbBr_3$ on Si/SiO_2 substrate, the AFM images revealed a thickness of ~ 20 nm and a roughness of ~ 5 nm within one printed line (Figure S4).

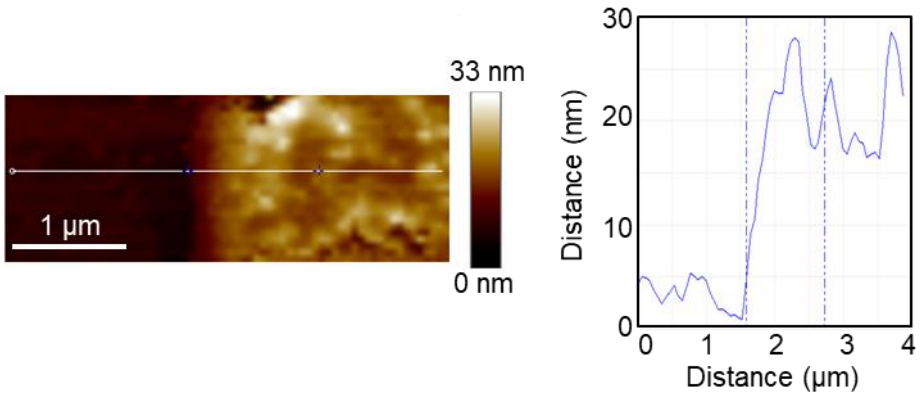

Figure S4 a) AFM image of the edge of 5 printed layers $CsPbBr_3$ film on Si/SiO_2 **b)** Height profile for the line indicated in the image (white line).

SI3. Electrical properties of CVD graphene devices

Mobility of CVD single layer graphene (SLG) devices were calculated from $\sigma_{sd}(V_g)$ dependence (Figure S4a) using the equation $\mu = \frac{\sigma_{sd}}{V_g}\frac{d}{\varepsilon_0\varepsilon}$ [S2]. Deposition of $CsPb(Br/I)_3$ NCs resulted in a hysteresis of $\sigma_{sd}(V_g)$ (Figure S5b), which depends on the direction of V_g sweep, as was previously observed for drop-cast NC decoration of graphene [S3]. After illumination, the electrical properties of the inkjet deposited $CsPbX_3$/SLG device recover to their original value (Figure S5c). ON/OFF temporal response of $CsPbBr_3$/SLG device (Figure S5d) with excitation and relaxation time constants of τ_{rise} = 1.5 s and τ_{fall} = 5.6 s, respectively.

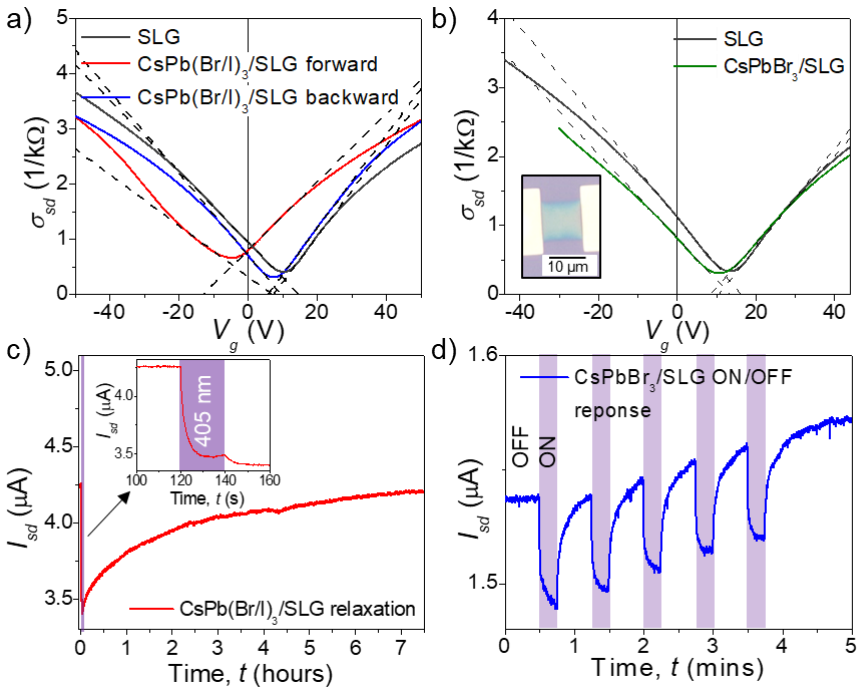

Figure S5. Gate voltage, V_g dependence of SLG conductivity, σ_{sd}, before and after inkjet deposition of **a)** $CsPb(Br/I)_3$ (V_{sd} = +5 mV) (V_g is swept from -50 V to +50 V and then back to -50 V with sweep rate of 0.1 V/s) and **b)** $CsPbBr_3$ (V_{sd} = +2 mV) NCs. (V_g is swept from -30 V to +45 V with sweep rate of 0.1 V/s). The dashed lines show linear fit of $\sigma(V_g)$ curves in the points of maximum filed effect mobility: negative V_g fits are used for calculation of hole mobility and positive V_g lines for electron mobility (see Method section for details) Inset: optical image of $CsPbBr_3$/SLG device **c)** Temporal response of $CsPb(Br/I)_3$/SLG device to illumination for 20s (λ_{ex} = 405 nm, P = 0.56 W/m^2, V_{sd} = +2 mV). **d)** ON/OFF temporal response of $CsPbBr_3$/SLG device (λ_{ex} = 405 nm, P = 0.56 W/m^2, and V_{sd} = +2 mV) with excitation and relaxation time constants of τ_{rise} = 1.5 s and τ_{fall} = 5.6 s.

The enhancement of the stability of the $CsPb(Br/I)_3$/SLG devices was assessed with respect to their electrical properties and photoresponse. Only a small decrease of photoresponsivity is observed (Figure S6).

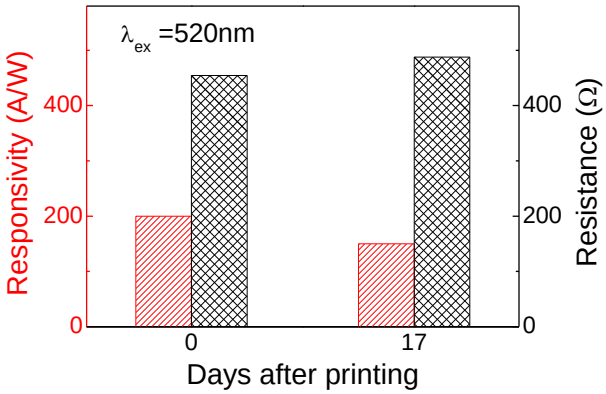

Figure S6. Responsivity (red bars; λ_{ex} = 520 nm, P = 5.6 mW/m^2) and resistance (black) of CsPb(Br/I)3 /SLG device on the day of printing (day 0) and after 17 days storage at ambient conditions.

SI4. $CsPbX_3$/SLG devices at different excitation energies

The photocurrent induced by incident light of different energies (E_{ex}) for the $CsPbX_3$/SLG devices is consistent with their respective absorption spectra (Figure S7).

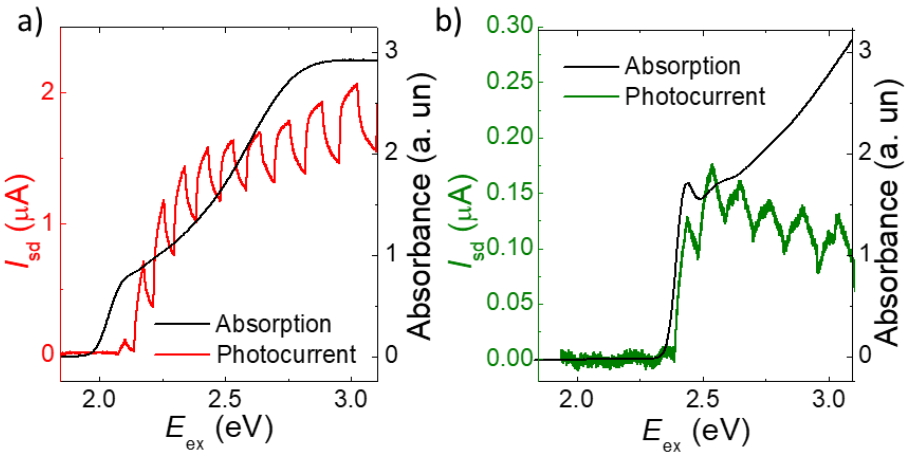

Figure S7. Dependence of photocurrent, I_{pc}, on the wavelength of incident light for **a)** the $CsPb(Br/I)_3$/SLG device (P ~ 0.03 W/m^2, V_{sd} = 10 mV) and **b)** the $CsPbBr_3$/SLG device (P ~ 0.3 W/m^2, V_{sd} = 5 mV), compared to their respective absorption spectra (black line).

SI5. Drop-cast $CsPb(Br/I)_3$ NCs on iGr

The temporal response of drop-cast $CsPb(Br/I)_3$ NCs on an iGr device under excitation with different wavelengths (Figure S8). The responsivity of the $CsPb(Br/I)_3$/iGr device decreases with increasing excitation energy from 520 nm to 405 nm (Figure S8). This is likely due to the large perovskite NC layer thickness caused by drop casting. The charge transfer between the NCs is negligible and only the layer of the NC directly adjacent to graphene contributes to the photocurrent [S3]. Since the absorption length of $CsPb(Br/I)_3$ demonstrates a considerable decrease with increasing photon energy [S3], high energy photons are mostly absorbed within a thin top layer of the $CsPb(Br/I)_3$ NC film.

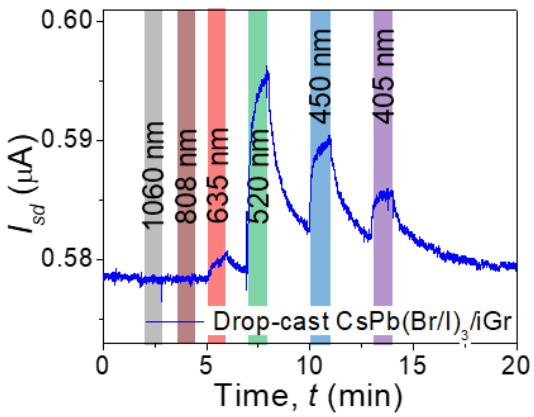

Figure S8. Temporal response of drop-cast $CsPb(Br/I)_3$ on an iGr device under illumination with different laser wavelengths (P = 0.56 mW/mm^2, V_{sd} = +10 mV).

SI6. Printed iGr-$CsPb(Br/I)_3$ hybrid

Photoresponse of 5-printed layer iGr-$CsPb(Br/I)_3$ hybrid annealed at 250 °C for 30 minutes, compared to the other printed $CsPb(Br/I)_3$ devices from this work (Figure S9).

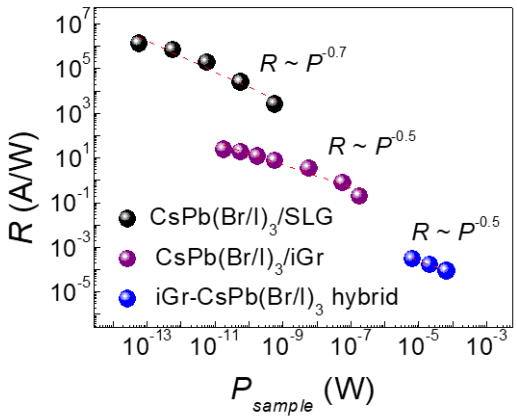

Figure S9 Photoresponsivity, *R*, versus power on the sample (λ_{ex} = 520 nm illumination) for the printed iGr-CsPb(Br/I)$_3$ hybrid device compared to other printed CsPb(Br/I)$_3$ detectors from this work.

SI7. Printed CsPb(Br/I)$_3$/iGr heterostructure

After inkjet deposition of 1 layer of CsPb(Br/I)$_3$ onto 1 layer of iGr, the sheet resistance, ρ_s, increased by ~10% (Figure S10), hence indicating intermixing between the layers.

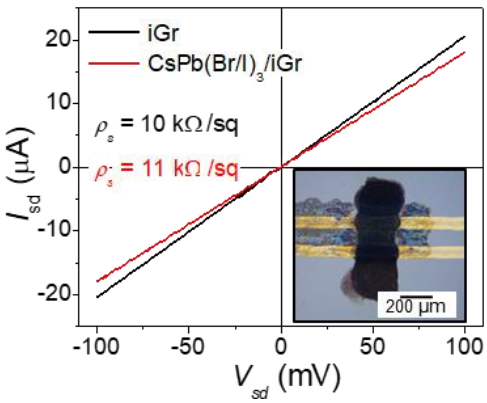

Figure S10. *I*(*V*) characteristics of 1 layer of iGr before and after inkjet deposition of CsPb(Br/I)$_3$ (1 layer) on top (sample area is 30 µm x 60 µm). Inset: image of printed CsPb(Br/I)$_3$/iGr heterostructure (10 layer CsPb(Br/I)$_3$, 3 layer iGr) with printed Au NP contact pads.

References

[S1] A. Gao, J. Yan, Z. Wang, P. Liu, D. Wu, X. Tang, F. Fang, S. Ding, X. Li, J. Sun, M. Cao, L. Wang, L. Li, K. Wang, X.W. Sun, Printable CsPbBr3 perovskite quantum dot ink for coffee ring-free fluorescent microarrays using inkjet printing, Nanoscale. 12 (2020). https://doi.org/10.1039/c9nr09651e.

[S2] S. V. Morozov, K.S. Novoselov, M.I. Katsnelson, F. Schedin, D.C. Elias, J.A. Jaszczak, A.K. Geim, Giant intrinsic carrier mobilities in graphene and its bilayer, Phys. Rev. Lett. 100 (2008). https://doi.org/10.1103/PhysRevLett.100.016602.

[S3] N.D. Cottam, C. Zhang, L. Turyanska, L. Eaves, Z. Kudrynskyi, E.E. Vdovin, A. Patanè, O. Makarovsky, Defect-Assisted High Photoconductive UV–Visible Gain in Perovskite-Decorated Graphene Transistors, ACS Appl. Electron. Mater. 2 (2020). https://doi.org/10.1021/acsaelm.9b00664.